

# On The Creation of Stagnation Points in a Rotating Flow.

T. Mullin, S. J. Tavener\* & K. A. Cliffe†  
Department of Physics and Astronomy,  
The University of Manchester,  
Manchester M13 9PL.

## Abstract

We report the results of a numerical study of the creation of stagnation points in a rotating cylinder of fluid where both endwalls are rotated. Good agreement is found with previous results where the stagnation points are formed on the core of the primary columnar vortex. Novel phenomena have been uncovered at small aspect ratios where stagnation occurs off-axis directly and the secondary vortex which is created forms a toroid. The case is then considered of a small cylinder placed along the centre of the flow and despite the qualitatively different boundary condition, the phenomena are found to be robust.

## 1 Introduction

The steady flow in a cylinder where one or both endwalls rotate has been the subject of a great deal of numerical and experimental research. The case where one endwall rotates was first studied by Vogel (1968) in a combined numerical and experimental investigation. He showed that the primary flow was a columnar vortex which developed a pair of stagnation points midway along its central core above a certain Reynolds number,  $Re$ . An axisymmetric secondary recirculation was thus created and Vogel suggested that this situation could be considered as a weak steady form of the important and yet

ill-understood problem of vortex breakdown. (See e.g. Hall (1972)). This interpretation of events is still not widely accepted (see e.g. Keller (1995)) and perhaps this focus of the debate detracts from what is an interesting internal vortex flow. It is appealing in that it is one of the few fluid mechanical situations where close quantitative comparison can be made between numerical calculation and experimental observation. It also has technological implications for a diverse range of flow situations such as swirl combustion chambers, flow between shrouded computer disks and in satellite fuel containers. In all of these situations, a deeper understanding of the origin and location of stagnation points could prove vital in gaining insight into the origins of time dependence and hence more complicated motions.

Vogel's original work was extended by Escudier (1984) who carried out a systematic experimental study. He established the range of existence of the secondary vortices in terms of the two control parameters  $Re$  and the aspect ratio,  $\Gamma$ . In particular, he showed that the secondary vortices exist over a finite range of  $Re$ , i.e. they appear above a certain value of  $Re$  and disappear above a greater one. He also showed that they do not form for  $\Gamma \leq 1.0$  and that multiple steady vortices and time-dependence exists at sufficiently large  $\Gamma$ , and  $Re$ .

Escudier's results have stimulated several numerical and experimental investigations. Perhaps the most extensive discussion of the phenomena are given in a series of papers by

---

\*Dept. of Mathematics, Penn. State University

†AEA Technology, Harwell

Lopez and his collaborators (1990a, 1990b, 1992). These results are broadly in agreement with Escudier's observations and the insight gained from the numerical investigation has been used to establish a criterion for the onset of the secondary recirculation. Further numerical investigations were performed by Tsitverblit (1993) who used continuation methods with the steady Navier Stokes equations to show that the secondary vortices do not appear critically at a bifurcation point but rather evolve smoothly with increase of  $Re$ .

In more recent investigations the focus of attention has moved towards variants of the original problem. These include counter and co-rotation of both ends of the cylinder by Jahnke and Valentine (1996) and Gelfgat, Bar-Yoseph and Solan (1996), flow with a free surface by Hyun (1985) and Spohn, Mary and Hopfinger (1993) and symmetric rotation of both ends by Valentine and Jahnke (1994). The counter and co-rotation of ends has been found to either suppress or enhance the secondary vortex respectively. It is the configuration where both ends co-rotate at the same speed which is the subject of our investigation, since it provides new and interesting features which are not present in the original problem of a singly rotated end.

Valentine and Jahnke's work was inspired by Spohn et al's experiments with a free surface. They show that by changing the end boundary from a stationary wall as in the original problem, to a free surface, so the upper limiting  $Re$  for the recirculation is removed. Their calculations are for the case where the aspect ratio is greater than one. Instead of disappearing as  $Re$  is increased, the recirculation intensifies and migrates from the central core to a point off-axis. Hence, the stagnation point becomes a circular stagnation line or periodic point of the flow and the recirculation bubble forms a torus. In Valentine and Jahnke's numerical model both ends rotate at the same speed so that the central plane is equivalent to the free surface of the experiment. Now, two

pairs of stagnation points are formed at sufficiently large  $Re$  so that a pair of recirculation bubbles are equally disposed about the mid-plane. It is established that there is no upper limit to the existence of the secondary recirculation bubbles and broad agreement between theory and experiment is obtained. In addition, the bubbles are also found to migrate from the core to off-axis locations as  $Re$  is increased, so that a toroidal bubble is formed and the stagnation points become periodic points of the flow as in the free surface experiments. These results were confirmed and extended to include the onset of time-dependence by Lopez (1995) for the symmetric driven ends case with aspect ratio 1.5.

The aim of the present study is to extend the parameter range studied by Valentine and Jahnke to include aspect ratios smaller than one where novel phenomena are uncovered. We study the steady, axisymmetric Navier Stokes equations using the numerical continuation program called ENTWIFE (Cliffe (1996)) which we have used extensively to obtain good quantitative agreement between calculation and experiment for Taylor-Couette flows (see e.g. Cliffe, Kobine and Mullin (1992)). The weight of numerical and experimental evidence suggests that the creation of the secondary recirculation is a steady axisymmetric phenomenon and hence this approach seems justified. We then consider the situation where a thin solid cylinder is placed along the central core. This qualitative change in the inner boundary condition is, perhaps surprisingly, shown to have little effect on the results. We consider the cases where the inner cylinder rotates with the endwalls and where it is stationary and compare and contrast the results. Finally, we investigate the effects of increasing the diameter of the inner cylinder to see if the phenomena persist into parameter regimes normally associated with Taylor-Couette flows.

## 2 Formulation of the problem and numerical technique

We computed steady, axisymmetric flows of an incompressible Newtonian fluid in bounded cylindrical or annular domains. The restriction to axisymmetric flows enabled the computations to be performed in two-dimensional (radial) domains, as shown in Figure 1. Superscripts (\*) denote dimensional quantities. Three different flow configurations were investigated. In each case the top and bottom surfaces rotated with the same angular velocity  $\Omega$ . We considered; (i) no inner cylinder (for which  $r_1^* = 0$ ), (ii) a stationary inner cylinder, and, (iii) an inner cylinder rotating with angular velocity  $\Omega$ .

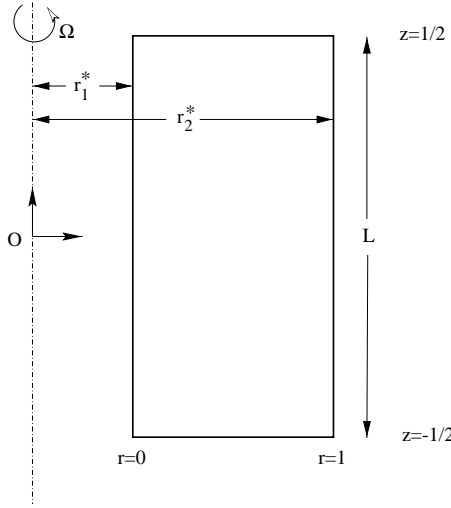


Figure 1: Schematic of the computational domain

The primitive variable formulation of the incompressible steady, axisymmetric Navier-Stokes equations was solved via the finite-element method, using quadrilateral elements with biquadratic interpolation of the velocity field and discontinuous piecewise linear interpolation of the pressure field. The length and velocity scales, and therefore the Reynolds number and aspect ratio, depended upon the problem at hand.

(i): *No inner cylinder.*

The natural length and velocity scales

were the radius of the container  $r_2^*$  and  $\Omega r_2^*$  respectively. The Reynolds number,  $R = \Omega (r_2^*)^2 / \nu$  and the aspect ratio,  $\eta = L^* / r_2^*$ . We defined  $r = r^* / r_2^*$ ,  $z = z^* / r_2^*$ ,  $u_r = u_r^* / \Omega r_2^*$ ,  $u_\theta = u_\theta^* / \Omega r_2^*$  and  $u_z = u_z^* / \Omega r_2^*$ . The computational domain was therefore

$$\{(r, z) \in [0, 1] \times [-0.5, 0.5]\}$$

and the boundary conditions were

$$\begin{cases} u_r = 0 \\ u_\theta = r, \text{ on } z = \pm 0.5 \\ u_z = 0 \end{cases}$$

$$\begin{cases} u_r = 0 \\ \frac{\partial u_\theta}{\partial r} = 0, \text{ on } r = 0 \\ \frac{\partial u_z}{\partial r} = 0 \end{cases}$$

$$\begin{cases} u_r = 0 \\ u_\theta = 0, \text{ on } r = 1 \\ u_z = 0 \end{cases}$$

(ii): *Stationary inner cylinder.*

The natural length and velocity scales were the gap width  $d^* = r_2^* - r_1^*$  and  $\Omega r_1^*$  respectively. The Reynolds number,  $R = \Omega r_1^* d^* / \nu$ , the aspect ratio,  $\eta = L^* / d^*$ , and the radius ratio  $\eta = r_1^* / r_2^*$ . We defined  $r = (r^* - r_1^*) / d^*$ ,  $z = z^* / d^*$ ,  $u_r = u_r^* / \Omega r_1^*$ ,  $u_\theta = u_\theta^* / \Omega r_1^*$  and  $u_z = u_z^* / \Omega r_1^*$ . The computational domain was again

$$\{(r, z) \in [0, 1] \times [-0.5, 0.5]\}$$

and the boundary conditions were

$$\begin{cases} u_r = 0 \\ u_\theta = 1 + \left(\frac{1-\eta}{\eta}\right) r, \text{ on } z = \pm 0.5, \\ u_z = 0 \end{cases}$$

$$\begin{cases} u_r = 0 \\ u_\theta = 0, \text{ on } r = 0, 1. \\ u_z = 0 \end{cases}$$

(ii): *Rotating inner cylinder.*

The length and velocity scales were the same as for (ii) and the same non-dimensionalization was applied. The boundary conditions were

$$\begin{cases} u_r = 0 \\ u_\theta = 1 + \left(\frac{1-\eta}{\eta}\right) r, \text{ on } z = \pm 0.5, \\ u_z = 0 \end{cases}$$

$$\begin{cases} u_r = 0 \\ u_\theta = 1, \text{ on } r = 0 \\ u_z = 0 \end{cases}$$

$$\begin{cases} u_r = 0 \\ u_\theta = 0, \text{ on } r = 1. \\ u_z = 0 \end{cases}$$

Most of the calculations were carried out using  $24 \times 28$  elements but some were also performed using  $48 \times 56$  elements to check details. No appreciable difference was found between the results. Appropriate corner refinement of the finite-element mesh and smoothing of the velocity discontinuities was employed. Details of both may be found in Tavener, Mullin and Cliffe (1990). Arclength continuation methods were used to follow solution branches in  $(R, \eta)$  parameter space. The streamfunction was computed from the primitive variable solution.

As pointed out by Tsitverblit (1993), the onset of the recirculation bubble is a continuous process and so an estimate of its appearance requires an extra criterion. This is not a straightforward procedure since the bubble is typically very weak compared with the primary vortex and the spatial location depends on  $\eta$ . The first point is often not commented on in the literature where streamlines for the primary and secondary vortices are most often plotted using non-uniform scaling to emphasise the bubble. This has the obvious advantage of enhancing the structure of the bubble but it may give a misleading impression of its strength. The effect of the weakness of the bubble is compounded by the varying spatial location of its onset and this rendered all attempts to automatically detect its appearance ineffective.

The method we used to detect the first onset of the bubble was to simply visually inspect the streamline plots calculated for fixed  $\eta$ , when Re was increased in  $\sim 1\%$  steps. A

bubble was deemed to be present when a visible area was first enclosed by the zero streamline. In practice, the bubble grows rapidly with Re and so we are confident that this is a reliable criterion which is robust. Moreover, our results are in good quantitative agreement with the limited data set available from Valentine and Jahnke (1994) who used alternative methods.

### 3 Results

The results for the boundary of the range of existence of the secondary recirculations on the  $(\text{Re}, \eta)$  plane for the case of no inner cylinder are shown in figure 2. We have decided to show the results as a series of points rather than a fitted curve to emphasise that these are estimates of the bubble onset obtained using the methods described above. For parameter values below the line of points labeled ABCD, only the primary vortex exists and the secondary recirculation bubbles form when this curve is crossed by varying either Re or  $\eta$ .

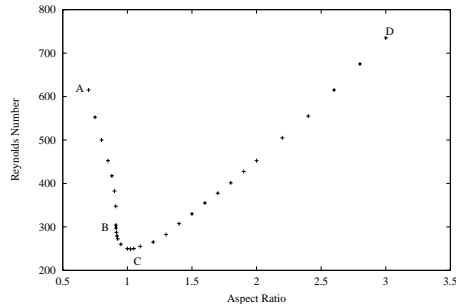


Figure 2: Plot of domain of existence of recirculation bubble on the  $(\text{Re}, \eta)$  plane. The bubble exists above the curve ABCD.

In the aspect ratio range C to D two pairs of stagnation points are formed on the core of the primary vortex. We show a typical sequence of streamline plots for this range of  $\eta$ , in figure 3. All the streamline plots are shown in the computational domain

$$\{(r, z) \in [0, 1] \times [-0.5, 0.5]\}$$

shown schematically in figure 1. This corresponds to one half of a cross-sectional slice

through the axisymmetric domain. We have chosen small streamline values to emphasise the bubble and hence omitted those for the primary vortex which are typically two to three orders of magnitude greater. They were calculated for  $\gamma = 2.0$  and (a)  $Re = 450$ , (b)  $Re = 455$  and (c)  $Re = 500$ . It can be seen that the recirculations appear on axis between  $Re = 450$  and  $455$  and subsequently increase in size and strength as  $Re$  is increased.

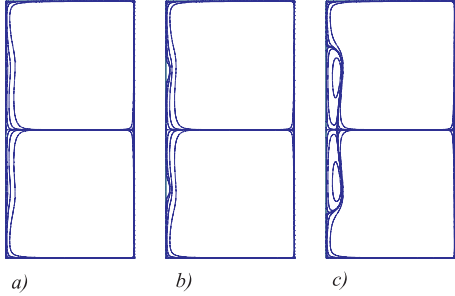


Figure 3: Half-plane streamline plots for  $\gamma = 2$  and (a)  $Re = 450$  (b)  $Re = 455$  and (c)  $Re = 500$ . In each case there is no inner cylinder present. In each figure  $\psi = \pm 1 \times E^{-7}$  to  $\pm 1 \times E^{-4}$  in steps of  $1 \times E^{-1}$  and 0.

The next sequence of streamline plots shown in figure 4 were calculated at  $\gamma = 0.8$  and (a)  $Re = 500$ , (b)  $Re = 505$  and (c)  $Re = 520$  and are typical of events at onset in the aspect ratio range A to C in figure 2. Distortion of the streamline patterns such as in figure 4(a), is first seen at  $Re \sim 450$ . However, flow reversal and the enclosure of a detectable area by the zero streamline is first evident at  $Re = 505$  as in figure 4(b). The recirculations now form a toroidal vortex whose inner and outer limits are set by circles of stagnation lines around the generator of the cylinder. Hence the stagnation points are now periodic points of the flow. These toroidal vortices have been reported previously by Valentine and Jahnke (1994) and Spohn et al (1993) but in those cases, the bubbles were initially formed on the core and they subsequently migrated to an off-axis position as  $Re$  was increased. We believe that the present results are the first calculations

of the direct onset of these toroidal vortices.

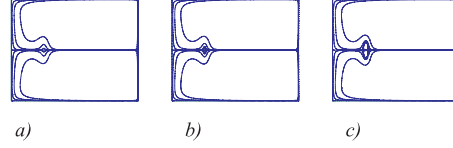


Figure 4: Half-plane streamline plots for  $\gamma = 0.8$  and (a)  $Re = 500$  (b)  $Re = 505$  and (c)  $Re = 520$ . In each case there is no inner cylinder present. In each figure  $\psi = \pm 1 \times E^{-7}$  to  $\pm 1 \times E^{-4}$  in steps of  $1 \times E^{-1}$  and 0.

In the aspect ratio range B to C in figure 2, a mixed stage is observed where there is a pair of stagnation points on the axis and a single circular stagnation line off-axis. Thus there is a smooth change in the type of recirculation bubble formed at onset involving the coalescence of pairs of stagnation points. For large  $\gamma$ , a pair of on-axis bubbles is formed at onset while for small  $\gamma$ , a toroidal vortex develops. It is clear that there is no lower limit to the aspect ratio range for the existence of these secondary vortices. These results are in agreement with the speculation of Spohn et al who suggested that this should be the case but were unable to pursue this point in their experimental investigation due to technical difficulties.

The above results show that stagnation points need not necessarily form initially on the central core of the flow. Indeed, Jahnke and Valentine (1996) have shown that separation may also occur on the outer boundary of the cylinder when it is made to rotate. All of this evidence suggests that if a small cylinder is placed along the central core of the flow then one might expect toroidal vortices to appear above a certain range of  $Re$ . We therefore decided to investigate this possibility and the results for the range of existence of these secondary vortices are shown in figure 5.

We studied two different versions of the problem. In one, the inner cylinder rotated with the ends while in the other it remained stationary. The set of points for the case where the inner cylinder rotates with the

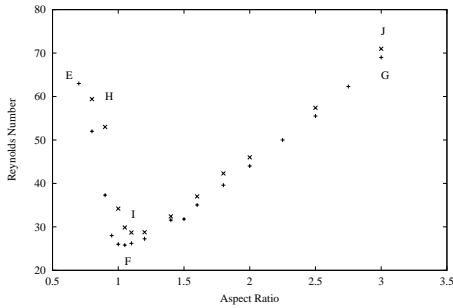


Figure 5: The range of existence of the recirculating bubbles with inner cylinders present plotted as a function of  $Re$  and  $\gamma$ . The locus labeled EFG is for a rotating inner cylinder and HIJ for a stationary one. In both cases the radius ratio is set to 0.1.

ends is labeled EFG while that for a stationary cylinder is labeled HIJ in figure 5. The radius ratio of the two cylinders was set to 0.1 for all of these calculations. It is immediately clear that they have the same qualitative form as each other and are also the same as the set shown in figure 2 where there is no inner cylinder present. The locus of points for the stationary cylinder case is above that for the rotating one indicating that rotation assists the onset of the recirculation bubble.

It may also be seen in figure 5 that the minima of the curves are all at approximately the same aspect ratio in all three cases. The scaling for  $Re$  now involves the radius of the inner cylinder and the gap width which is the convention for Taylor-Couette flows. Hence the ratio of this Reynolds number and that defined for the case when no inner cylinder is present involves

$$\eta(1 - \eta).$$

Thus the minimum for the case of a rotating cylinder would be  $\approx 28.0$  and that for a stationary one is  $\approx 32.0$ . Hence in the cases where an inner cylinder is present the minimum is  $\sim 10\%$  of the corresponding value for no cylinder.

We show in figures 6 and 7 the streamline sequences for the onset of the bubbles for aspect ratios 2 and 0.8 where a rotating inner cylinder is present. The sequences for

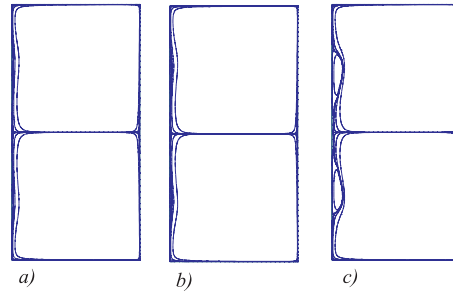


Figure 6: Half-plane streamline plots for  $\gamma = 2.0$  and (a)  $Re = 43$  (b)  $Re = 44$  and (c)  $Re = 50$ . In each case a rotating cylinder is present at the left hand edge of the figure. In each figure  $\psi = \pm 1 \times E^{-7}$  to  $\pm 1 \times E^{-4}$  in steps of  $1 \times E^{-1}$  and 0.

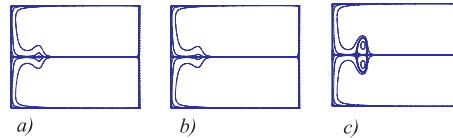


Figure 7:  $Re = 52$  and (c)  $Re = 60$ . In each case a rotating cylinder is present at the left hand edge of the figure. In each figure  $\psi = \pm 1 \times E^{-7}$  to  $\pm 1 \times E^{-4}$  in steps of  $1 \times E^{-1}$  and 0.

a stationary inner cylinder exhibit the same features except that they are displaced to slightly higher Reynolds numbers. It can be seen that the streamline patterns are qualitatively similar to those shown in figures 3 and 4 when there was no inner cylinder present. A pair of toroidal recirculation bubbles are formed near the inner cylinder at the larger value of  $\gamma$ , and as an off-axis toroidal vortex for  $\gamma = 0.8$ . The formation sequence shown in figure 6 is perhaps less distinct than in the case when there is no cylinder present but when viewed in detail it can still be distinguished. Hence, the addition of a small cylinder has not produced any qualitatively different features. There are some weak effects but they are subtle and will require more research before any definite statements can be made.

We now turn our attention to the effect of the radius ratio of the two cylinders on the onset of the stagnation points in these rotat-

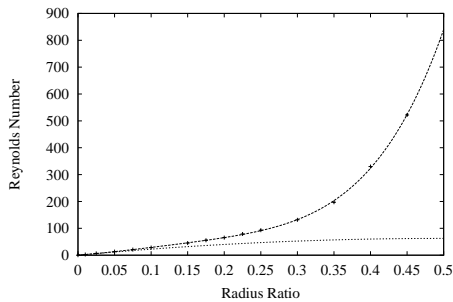


Figure 8: Graph of the onset Reynolds number for a recirculation bubble for aspect ratio 1.0 plotted as a function of radius ratio. A curve has been fitted to the calculated points. The lower curve shows the relationship  $250\eta(1 - \eta)$ .

ing flows. This investigation was carried out using the case where the inner cylinder rotates with the ends. We show in figure 8 the Reynolds number for the onset of the bubble at  $\gamma = 1$  plotted as a function of the radius ratio  $\eta$ . A curve has been fitted through the calculated data points using least squares. It can be seen that the Reynolds number for onset is greatly affected by  $\eta$  and rises steeply as  $\eta \rightarrow 0.5$ . At these Reynolds numbers in Taylor-Couette type flows a strong time dependence would occur and so it is unlikely that they will be observable in an experiment. However, flows with similar vortex structure have been found in Taylor-Couette and related flows by Lensch (1988) and Kobine and Mullin (1994). Both cases involved experiments with a single primary vortex which developed a small secondary vortex above a certain range of Reynolds numbers. Hence the situation is analogous to the present one but the relationship plotted in figure 8 suggests that any link may be coincidental.

The lower curve shown in figure 8 was obtained using the relationship  $250\eta(1 - \eta)$  which should hold if there is a simple scaling between the case with no cylinder and the present one. If the onset of the bubble is unaffected by the presence of the cylinder the Reynolds numbers with and without the inner boundary should have a simple ge-

ometrical relationship. It can be seen that this is a reasonable approximation for values of  $\eta \leq 0.1$  and thereafter the inner cylinder has a strong effect on the flow field.

## 4 Conclusions

The numerical results reported here agree with previous calculations and observations for the onset of recirculation bubbles within internal rotating flows. We have extended the investigation to small aspect ratios and found the first evidence for the direct onset of off-axis toroidal bubbles which ought to be observable in an experiment. We have also shown that the flow is relatively insensitive to qualitative changes in the inner boundary condition which were achieved by introducing solid cylinders along the central axis. This is true as long as the radius ratio of the two cylinders is less than 0.1.

## Acknowledgements

We are grateful to Pedro Reis for help with preparing the manuscript.

## References

- BROWN, G. L. AND LOPEZ, J. M. 1990 "Axisymmetric vortex breakdown. Part2. Physical mechanisms," J. Fluid Mech. **221**, 553.
- CLIFFE, K. A. 1996 "ENTWIFE (Release 6.3) Reference Manual: ENTWIFE, INITIAL DATA and SOLVER DATA Commands," AEAT-0823.
- CLIFFE, K. A., KOBINE J. J. AND MULLIN T. 1992 "The role of anomalous modes in Taylor-Couette flow" Proc. Roy. Soc. Lond. A **439** 341.
- ESCUDIER, M. P. 1984 "Observations of the flow produced by a rotating end wall," Exp. Fluids **2**, 189.
- GELFGAT, A. Y., BAR-JOSEPH, P. Z. AND SOLAN A. 1996 "Steady states and oscillatory instability of swirling flow in a cylinder with rotating top and bottom" Phys. of

HALL, M. G. 1972 "Vortex breakdown" *Ann. Rev. Fluid Mech.* **4** 195.

HYUN, J. M. 1985 "Flow in an open tank with a free surface driven by the spinning bottom." *J. Fluid Eng.* **107** 495.

JAHNKE, C. C. AND VALENTINE, D. T. 1996 "Boundary layer separation in a rotating container," *Phys. of Fluids* **8** 1408.

KELLER, J. J. 1995 "On the interpretation of vortex breakdown," *Phys. of Fluids* **7** 1695.

KOBINE, J. J. 1994 "Low-dimensional bifurcation phenomena in Taylor-Couette flow with discrete azimuthal symmetry," *J. Fluid Mech.* **275** 379.

LENSCH, B. 1988 "Über die Dynamik der Einwirbelströmung im Taylor-Zylinder," Diplomarbeit, University of Kiel, Germany.

LOPEZ, J. M. 1990 "Axisymmetric vortex breakdown. Part 1. Confined swirling flow," *J. Fluid Mech.* **221**, 533.

LOPEZ, J. M. 1995 "Unsteady swirling flow in an enclosed cylinder with reflectional symmetry," *Phys. Fluids* **7**, 2700.

LOPEZ, J.M. AND PERRY, A.D. 1992 "Axisymmetric vortex breakdown. Part 3. Onset of periodic flow and chaotic advection," *J. Fluid Mech.* **234** 449.

SPOHN, A., MORY, M. AND HOPFINGER, E.J. 1993 "Observations of vortex breakdown in an open cylindrical container with a rotating bottom," *Exp. in Fluids* **14**, 70.

TAVENER, S. J. , MULLIN T. AND CLIFFE K. A. 1991 "Novel bifurcation phenomena in a rotating annulus" *J. Fluid Mech.* **229** 483.

TSITVERBLIT, N. 1993 "Vortex breakdown in a cylindrical container in the light of continuation of a steady solution," *Fluid Dyn. Res.* **11** 19.

VALENTINE, D.T. AND JAHNKE, C.C. 1994 "Flows induced in a cylinder with both end walls rotating," *Phys. of Fluids* **6**, 2702.

VOGEL, H. U. 1968 "Experimentelle Ergebnisse über die laminare Strömung in einem zylindrischen Gehäuse mit darin rotierender Scheibe," Max-Planck-Institut für Strömungsforschung, Göttingen, Bericht

